

IR DESIGN ISSUES FOR HIGH LUMINOSITY AND LOW BACKGROUNDS*

M. K. Sullivan†, SLAC National Accelerator Laboratory, Menlo Park, CA, USA

Abstract

New e^+e^- collider designs use high beam currents (>1 A) to help obtain a high luminosity value. This leads to several issues that affect detector background levels. I will discuss several of these issues and indicate some of the backgrounds the detectors at these new colliders will encounter. The experience of the first two B-factories (PEP-II and KEKB) and also of the currently operating SuperKEKB accelerator will be used and the discussion will also include the new Electron-Ion Collider to be built at Brookhaven National Laboratory.

INTRODUCTION

The first e^+e^- collider was the storage ring AdA built by Bruno Touschek at the INFN laboratory at Frascati in the early 1960s. This was the first of many matter anti-matter colliders. The late 1960s and early 1970s saw the construction and commissioning of several new e^+e^- colliders. SPEAR at SLAC, Menlo Park, ADONE at INFN Frascati, DORIS at DESY, Hamburg. VEPP-2 and VEPP-2M at BINP, Novosibirsk followed in the late 1970s. The early 1980s had PEP at SLAC and PETRA at DESY. These accelerators were at the e^+e^- energy frontier for new particle searches at that time. It was thought that the PEP and PETRA storage rings with E_{cm} energies of 29 GeV for PEP and 32-48 GeV for PETRA would discover the top quark which had an expected mass at the time of about 15 GeV. Cornell University started up CESR in 1979 as a new e^+e^- collider with an E_{cm} energy range of 3.5 to 12 GeV. This machine was the first of several more accelerators to specialize in producing B mesons.

A new e^+e^- collider called TRISTAN started up in 1987 at KEK in Tsukuba, Japan with an initial beam energy of 25 GeV (50 GeV E_{cm}). In only a few years it was upgraded to a beam energy of 32 GeV. No top quark was seen but the experiments at TRISTAN confirmed the gluon first seen by PETRA experimental detectors and also measured the vacuum polarization effect of the electron. The accelerator also was a pioneer in the use of super-conducting cavities for electron storage rings along with CESR and PETRA. Shortly after TRISTAN turned on, two other e^+e^- colliders, the SLC at SLAC and LEP at CERN, Geneva, specializing in the production of the Z resonance (91.2 GeV E_{cm}) and further studies of the WW threshold (160 GeV E_{cm}) by LEP.

The 1990s saw the construction and commissioning of two new e^+e^- colliders concentrating on generating high luminosity at the Upsilon (4S) resonance (10.56 GeV) in order to produce very large samples of B mesons. The design luminosity values were 5-30 times higher than anything that had been achieved to that point.

In order to achieve these high design luminosities, both asymmetric-energy B-factory designs (PEP-II and KEKB) used a separate storage ring for each beam and then filled each ring with as many bunches as possible. This led to the first high-current (greater than 1A) collider storage rings. It should be stated that, at this time, INFN in Frascati also built and commissioned a high-current double ring collider (DAΦNE) designed for specialized studies of the ϕ resonance (1.02 GeV) [1-2].

HIGH-CURRENT BEAMS

The asymmetric-energy B-factories (PEP-II and KEKB) achieved and collided multi-ampere beams. The PEP-II B-factory at SLAC reached beam currents of 1.9 A for the 9 GeV electrons and 2.9 A for the 3.1 GeV positrons and the KEKB machine achieved 1.1 A in the 8 GeV electron ring and 2.6 A in the 3.5 GeV positron ring.

The B-factories encountered and solved many issues related to these high-current beams. To name a few: High-Order Mode (HOM) heating, high synchrotron power in the arcs and subsequent beam pipe outgassing, coupled bunch instabilities, synchrotron radiation backgrounds in the detector, and general beam-related backgrounds in the detector as well as the onset of backgrounds related to the collision.

The success of the B-factories has led to the design of future accelerators that implement the use of high-current storage rings as a way of achieving high luminosity design values.

NEW COLLIDER DESIGNS

Here, I touch upon some of the new collider designs that employ high-current storage rings of either electrons and/or positrons. All of the machines mentioned below are described in greater detail in presentations at this workshop. I have selected a few of the design parameters for this discussion. The first machine is an already running accelerator, SuperKEKB.

SuperKEKB

This accelerator is an upgrade of the previous B-factory machine KEKB. KEKB achieved a luminosity of $2.11 \times 10^{34} \text{cm}^{-2}\text{s}^{-1}$ the world record at that time [3]. SuperKEKB is aiming to achieve a peak luminosity of $5\text{-}6 \times 10^{35} \text{cm}^{-2}\text{s}^{-1}$, 30 times higher than KEKB. SuperKEKB uses a new idea called the “nanobeam” colliding scheme [4] in which the crossing angle is large, and

* Work supported by the U.S. Department of Energy, Office of Science, Office of Basic Energy Sciences, under Contract No. DE-AC02-76SF00515 and HEP.

† sullivan@slac.stanford.edu

the actual collision area is much shorter than the bunch length. This allows one to reduce the β_y^* value well below the bunch length and thereby gain more luminosity. The accelerator design calls for stored beam currents of 3.6 A for the 4 GeV positrons and 2.6 A for the 7 GeV electrons.

This accelerator is in the commissioning stage and has achieved a new world record luminosity of $4.65 \times 10^{34} \text{cm}^{-2}\text{s}^{-1}$ [5]. In addition, the stored beam current of each ring is over 1 A and they have demonstrated that the nanobeam colliding scheme does work.

FCC-ee and CEPC

These two designs are very similar and hence are considered together here. The FCC-ee design is an e^+e^- collider to be built at CERN with a 91 km tunnel circumference that contains two storage rings and a booster ring. The CEPC design has a 100 km circumference tunnel. Both machines intend to run over a range of stored beam energies. They will operate with beam energies of 45.6 GeV (Z resonance), 80 GeV, (W^+W^- threshold), 120 GeV, (ZH threshold), and 182.5 GeV (ttbar threshold). The point of interest for this discussion is the Z resonance running where both machines will employ high beam currents (1.4 A for FCC-ee and 0.8 A for CEPC) in order to achieve high design luminosities of $1.8 \times 10^{36} \text{cm}^{-2}\text{s}^{-1}$ for the FCC-ee design and $1.2 \times 10^{36} \text{cm}^{-2}\text{s}^{-1}$ for the CEPC design [6, 7].

Electron Ion Collider

A new electron-ion collider (EIC) is being designed to be built at BNL using some of the infrastructure of the RHIC collider together with a new electron storage ring and an electron booster ring. This machine plans to extend the physics found at HERA concerning the structure of the proton and develop a deeper understanding of the QCD model for the proton. The electron beam will operate at three energies: 5 GeV, 10 GeV and 18 GeV. The 18 GeV running has a maximum beam current of 0.27 A limited by available RF power and by a design maximum SR power limit on the ring of 10 MW [8, 9]. Of more interest in this discussion is the 10 GeV running condition where the design beam current is 2.5 A. This will put the electron storage ring into the B-factory parameter region and will be the highest design value for this beam energy.

NON-GAUSSIAN BEAM TAILS

One of the primary issues faced by all e^+e^- collider designs is the non-gaussian or halo beam tail distribution. The non-gaussian part of the transverse beam profile is the result of beam particle interactions which impart a transverse kick to the beam particle. There are a large number of sources for this type of interaction. Here we identify a few of these sources:

Beam-gas interactions [10] This interaction which is a beam particle colliding with a residual gas molecule in the beam pipe is very important in the early running of a collider and is usually the dominant source for the non-gaussian beam tail distribution during commissioning. Collimators can be used to reduce the beam tail particle density out

at high beam sigma values, but this will tend to reduce the beam lifetime to values that can be too low to maintain. Detector backgrounds are subsequently high at this time from both off-energy beam particles resulting from the collision and from excess synchrotron radiation from the beam particles with high beam sigma trajectories through the final focus magnets.

Particle-particle interactions inside a beam bunch.

Touschek scattering is one, inter-beam scattering (IBS) is another [11]. Touschek scattering is generally more significant for lower energy storage rings, but it can become important if the vertical emittance and subsequently the vertical size of the beam becomes small. This interaction increases as the particle density in a single beam bunch increases. One of the primary ways used to increase luminosity is to minimize the vertical size of the beam. This technique is being used for the SuperKEKB accelerator and consequently Touschek scattering is recognized as a primary source of detector background and as a contributor to shortening the beam lifetime.

Collision interactions. Here we have several sources contributing to the beam tails. The first one is Bhabha scattering [12]. This is the cross-section used to measure the luminosity of the collision. The design luminosity of the SuperKEKB is high enough to make this the dominant term that sets the design beam lifetime at a few minutes. The second-order interaction of radiative Bhabhas [12] also contributes to the non-gaussian beam tail as well as the shortness of the beam lifetime. This interaction also produces a spectrum of high-energy gammas that travel primarily down the beam axis defined at the collision point and these photons will strike the beam pipe at or near the first major bend after the collision. Beamsstrahlung, the emission of photons from the bending of the beam particles during collision, is another beam tail contributor [13]. This process becomes much more important as the beam energy increases and as the luminosity increases.

Instabilities. If a beam happens to be close to an instability threshold, then particles in the beam can be perturbed out of the gaussian distribution and into the beam tail distributions. This is also true if the ring gets too close to a resonance in the tune plane or if the tune shift from the collision pushes beam particles onto a resonance line. If the disturbance is too strong, then the beam lifetime is severely affected, and the beam can be lost. Generally, one steers away from tune plane resonances and tries to stay below instability thresholds, but other issues, like the dynamic pressure in the storage ring can sometimes lower some instability thresholds. This is also true for the Transverse Mode Coupled Instability (TMCI) where parts of the beam pipe (like collimator jaws) are positioned too close to the beam and generate wake-fields that are strong enough to influence the next bunch in the bunch train. Electron cloud interactions can also perturb the beam particles and even if the core gaussian is relatively untouched beam particle and electron cloud interactions can push some of the beam particles into the tail distributions.

BEAM TAIL MODELING

We see from the above, that there are a large number of sources that can populate a non-gaussian beam tail distribution. In general, *any* perturbation of the beam particles will do this. In addition, many of these sources are time dependent making it difficult to properly model the various sources. Some sources are more important at the beginning of a fill and others can become more important as attempts are made to improve the machine performance, such as adjusting the tunes or adjusting the collimators. The B-factories pioneered the technique of continuous top-up where the ring currents are kept steady by constantly injecting (usually at a rate of tens of Hertz) bunches into the stored rings. This greatly improves the machine performance since many factors stabilize when the beam currents are steady allowing the operators to concentrate on optimizing luminosity and performance.

With all this, the realistic modelling of the non-gaussian beam tail becomes problematic. I have chosen to model the tail distributions as another gaussian distribution but with a sigma that is several times larger than the core gaussian sigma. The x and y transverse dimensions are allowed to have different tail sigma values, but the height of the tail distributions is constrained to be the same value which is typically much smaller than the core height. The integral of the total tail distribution should be less than 10% of the core integral [14] and a more typical value used for modelling is 1-5% of the core integral.

Equation (1) is the differential form of the transverse beam particle distribution used for the synchrotron radiation background calculations in the program SYNC_BKG.

$$\frac{d^2N}{dxdy} = \exp\left[-\frac{x^2}{2\sigma_x^2} - \frac{y^2}{2\sigma_y^2}\right] + A_x A_y \exp\left[-\frac{B_x^2 x^2}{2\sigma_x^2} - \frac{B_y^2 y^2}{2\sigma_y^2}\right] \quad (1)$$

The equation includes the non-gaussian beam tail distributions for the X and Y dimensions. The σ_x and σ_y variables are the core σ values. The A_x , A_y , B_x , and B_y values determine the beam tail distributions with respect to the core distribution. As mentioned above, A_x and A_y are constrained to have the same value by choice, and they define the height of the tail distribution with respect to the core height. The B values determine the width of the tail distribution as a divisor to the respective core sigma.

Table 1 is a list of non-gaussian beam tail distribution A and B parameters for three different cases of beam tails, used to model the backgrounds observed in the partial PXD detector of Belle II during the initial commissioning of the SuperKEKB in 2019 and right after the roll-on of Belle II. Figure 1 (top) and (bottom) show the transverse profile of the beam including the three different beam tail distributions shown in parameter list from Table 1. The tail distributions are normalized to the core distribution where the maximum of the core distribution is one.

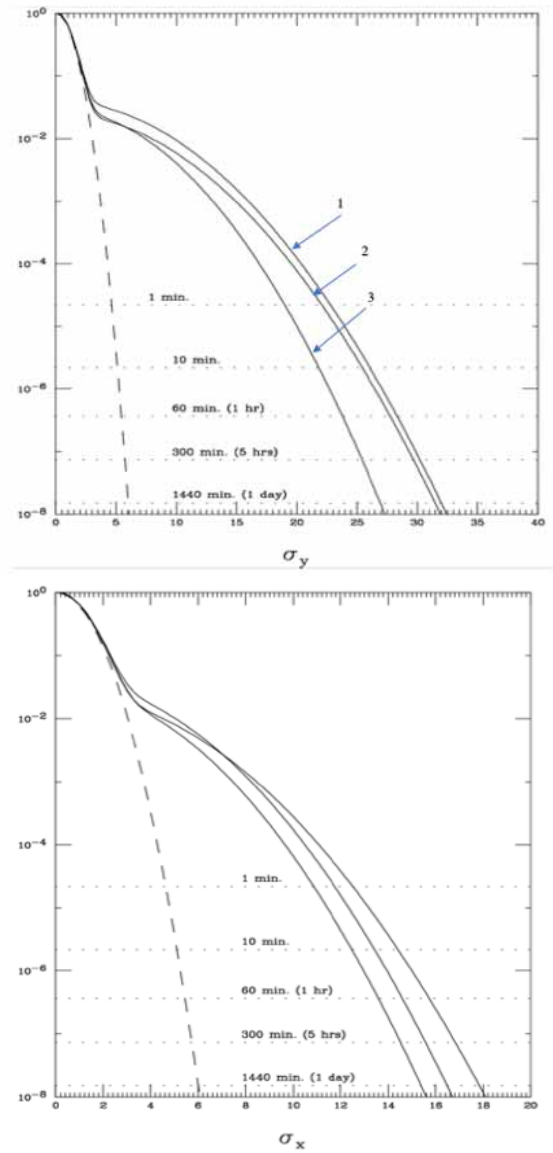


Figure 1: Top: The transverse beam profile in the X plane with the three different beam tail distributions listed in Table 1. The core gaussian distribution is shown as a dashed line and the non-gaussian beam tail distributions are shown as solid lines. Bottom: The transverse beam profile in the Y plane with the three different beam tail distributions listed in Table 1.

Table 1: List of non-gaussian beam tail distribution A and B parameters for three different cases of beam tails.

Beam Tail	A_x	B_x	A_y	B_y	%core
1	0.04	0.33	0.04	0.17	2.7
2	0.025	0.30	0.025	0.17	1.2
3	0.03	0.35	0.03	0.20	1.3

The modelling of the beam tail distribution can be further constrained by knowing the approximate beam lifetime and the value of the collimator settings at the time the background data was taken. This information can be used to set the particle density value at the setting of the collimator(s). Figure 1 (top) and (bottom) have dotted horizontal lines with time labels. These represent the estimated lifetime of the stored beam if a collimator setting is located at the intersection of the beam tail distribution with the dotted line. These lifetime estimates are based on a calculation for beam lifetime by M. Sands [15]. As an example, if an X collimator has a setting at 15σ then the lifetime of the beam should be a little over 300 min for tail distribution #3, about 60 min for #1, and 10 min for #2.

Backgrounds in the detector from synchrotron radiation can come from upstream bend magnets and from upstream quadrupoles. Usually, the bend radiation can be masked away from the detector beam pipe and the backgrounds from this source can be made low. The final focus quadrupoles also generate synchrotron radiation, and this is where the beam tail distribution becomes important. The number of beam particles out at high beam sigma values determines how much background the detector will get from this source. For flat beam designs the distribution in the X plane becomes the most important as flat beam designs have the vertical focusing quadrupole as the last magnet before the Interaction Point (IP). This puts the horizontally focusing magnet outside of the vertically focusing magnet forcing the horizontal magnet to over-focus in X because the vertically focusing (horizontally defocusing) magnet will remove some of the X focusing. The focus of both magnets needs to converge at the IP.

LUMINOSITY

When the luminosity is a few $\times 10^{33} \text{ cm}^{-2} \text{ s}^{-1}$ or higher for e^+e^- colliders and $e\text{P}$ colliders, the collision begins to add additional sources that contribute to the overall detector background level. One of these new sources is radiative Bhabha scattering where the interaction generates a high-energy (GeV) gamma ray that travels down the collision axis and an off-energy beam particle (electron or positron). The gamma rays will travel with the beam until the beam enters a dipole magnet. The gammas will then strike the beam pipe wall either inside the dipole magnet or else soon after exiting the magnet. This can be a source of neutron background as well as a source of shower debris from the showering gamma rays. The off-energy beam particle will be over-focused in the outgoing quadrupoles causing many of these particles to crash into the local beam pipe and generate shower debris in the detector. In addition, the first bend field encountered by the outgoing beam will bend many of the off-energy particles into the beam pipe wall. Both B-factories had outgoing bend fields that were relatively close to the collision point. The first PEP-II bend magnet started about 20 cm from the collision point and was one of the strongest bend fields in the entire accelerator. The first outgoing KEKB bending fields were about 2m downstream of the collision point. The close and strong bend field in the PEP-II B-factory produced a noticeable

radiative Bhabha background in the detector at a lower luminosity ($2-3 \times 10^{33}$) than for the KEKB machine which eventually began to see backgrounds from this source at a luminosity closer to 10^{34} . Figures. 2 and 3 illustrate the trajectories of these off-energy beam particles based on the energy of these beam particles after the radiative interaction and on the quadrupole and dipole fields in the interaction region.

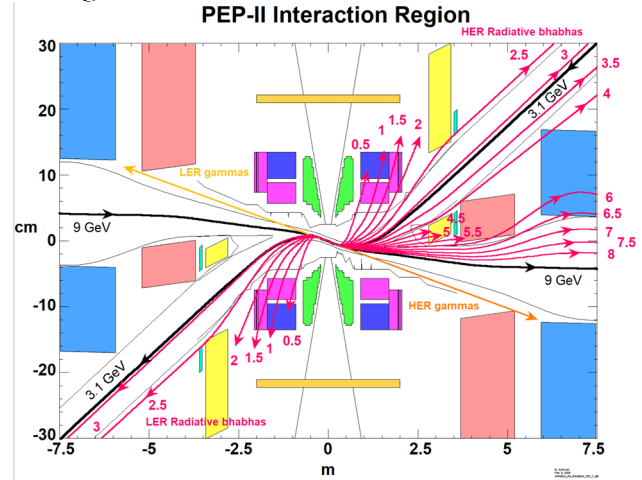


Figure 2: Layout of the PEP-II B-factory interaction region showing the trajectory of off-energy beam particles from a radiative Bhabha interaction. The gamma rays travel in a straight line away from the collision point and strike the beam pipe about 8 m downstream of the collision just outside of the blue X focusing magnet shown in the picture. The red trajectories and labels indicate the path and energy of the off-energy beam particle.

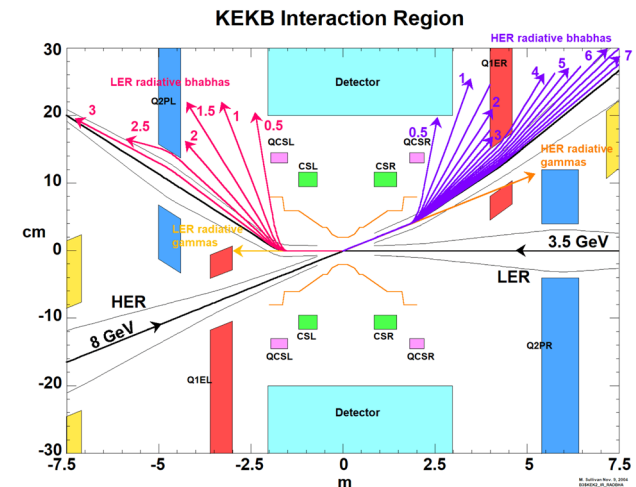


Figure 3: Layout of the KEKB B-factory interaction region showing trajectories of the off-energy beam particles after a radiative Bhabha interaction. The first strong bending fields in this design come from the outgoing beam traveling through a shared quadrupole magnetic field with a large off-axis trajectory. The incoming beams are on axis in these magnets. In the KEKB design, the gamma rays strike the beam pipe closer to the collision point than in the PEP-II design (approx. 2 m from the collision).

The SuperKEKB accelerator and all future collider designs discussed here have no shared quadrupole magnets. As mentioned in the figure caption, these are quadrupoles where both beams travel through the same magnetic field forcing at least one of the beams to be off axis in the quadrupole and thereby putting that beam into a strong bending field. In addition, SuperKEKB has moved the first bend magnet as far as possible from the IP as has all future collider designs. In spite of these efforts, background generated from radiative Bhabhas is still one of the highest detector backgrounds at the design luminosity of $5\text{--}6 \times 10^{35} \text{cm}^{-2}\text{s}^{-1}$ for Belle II.

Two-photon Interactions

Another luminosity related interaction that can cause detector background is called the low-energy e^+e^- pair production or the two-photon process. Here two virtual photons interact to create an e^+e^- pair of low energy particles. The Feynman diagram in Fig. 4 illustrates this process.

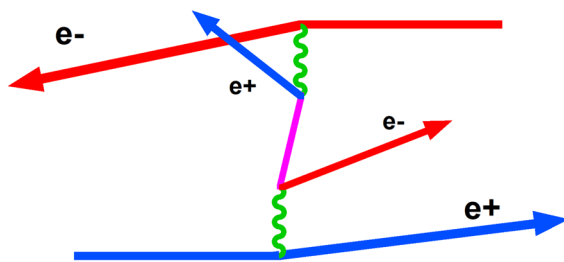


Figure 4: Feynman diagram of the interaction where an e^+e^- pair is produced. The low energy particles tend to have a trajectory that is a tight orbit around the detector axis due to the magnetic field of the detector.

Since the created particles have low energies, they will spiral around the detector magnetic field axis. As long as the particles remain inside the beam pipe this is not an issue. However, as the luminosity increases, this process will make e^+e^- pairs that have enough energy to go through the beam pipe and start spiralling through the vertex detector usually located very close to the central Be beam pipe. This generates an enormous number of hits in the vertex detector, and this can limit the detector performance. Consequently, this process can be a determining factor in how small the central beam pipe radius can be.

Beamsstrahlung

This interaction [13] is the emission of gamma rays at the collision point due to the bending of the beam particles from the entire electromagnetic fields of the other beam bunch. This was first studied for linear colliders where the collision focusing is quite intense and consequently this interaction plays an important part of the overall beam disruption parameter. Now, future collider designs also have to take this interaction into account, especially the FCC-ee and CEPC e^+e^- colliders when the accelerators are running at the Z pole (91.2 GeV) with very high beam currents. This process generates a very intense, high-power beam of

gamma rays along the outgoing beam axis that must be controlled and absorbed.

SUMMARY

The new accelerator designs that use multi-ampere stored beams to attain high luminosity will move accelerator and storage ring technology farther into the new territory first touched upon by the B-factories. The heavy synchrotron radiation power loads in the arcs of these machines will require some time to fully “scrub” the vacuum chamber and reduce the dynamic vacuum pressure before the design beam currents can be reached. In addition, the high design luminosity values means that the actual beam collision will become a major source of background for the detector. The stored beam lifetime for these machines with very high luminosity goals can become dominated by the loss of beam particles due to the collision. Electron (and positron) storage rings have a very strong damping term in the synchrotron radiation losses around the ring. This powerful damping term allows beam particles to be perturbed out of the core gaussian distribution of the beam into the transverse beam tails or halo distribution in a quasi-stable manner. As the SR damping draws these beam particles back into the core the perturbing mechanisms continue to repopulate the halo distribution. Any perturbation can kick some of the core particles out onto the tail distribution.

CONCLUSION

I have tried to describe what to me will be some of the new operating conditions we will encounter in the new high-current running and in some of the future e^+e^- colliders. There are clearly many important topics not discussed here that also impact interaction region designs (i.e. High-Order Mode effects for one). I suspect that even with all of our present knowledge of colliders and also of high-current storage rings we will still encounter new and unexpected issues related to high-current stored beams and to the increased luminosity design goals in the present and new machines. But then that is what makes pushing into new territory interesting and exciting.

ACKNOWLEDGEMENTS

I wish to acknowledge the design teams from the Thomas Jefferson National Accelerator Laboratory and the Brookhaven National Laboratory for the many discussions concerning the electron high-beam current plan for the EIC. I also want to acknowledge the design teams for the FCC-ee and for the CEPC for many fruitful meetings and discussions concerning the detector backgrounds and the interaction region design. Last, but by no means least, I wish to thank the SuperKEKB and Belle II accelerator and detector background teams for their many discussions and presentations of running conditions in the process of commissioning and understanding the new accelerator and detector.

REFERENCES

- [1] The information in the introduction came mostly from the website:
<https://en.wikipedia.org/>.
In particular, the links:
https://en.wikipedia.org/wiki/Particle_accelerator,
and
https://en.wikipedia.org/wiki/List_of_accelerators_in_particle_physics
as well as information concerning specific accelerators on individual web pages by the name of or the acronym for the accelerator.
- [2] A.Sessler, E. Wilson, “Engines of Discovery”, *World Scientific Publishing Co.*, 2007.
- [3] Y. Funakoshi, “Luminosity Tuning at KEKB”, in *Proc. eeFACT’16*, pp. 147-150, paper TUT3BH3, 2016.
- [4] SuperB Collaboration, “SuperB Conceptual Design Report”, INFN/AE-07/2, arXiv:0709.0451 [hep-ex], 2007.
doi:10.48550/arXiv.0709.0451
- [5] Y. Funakoshi *et al.*, “The SuperKEKB has Broken the World Record of the Luminosity”, in *Proc. IPAC’22*, Bangkok, Thailand, Jun. 2022, pp. 1–5.
doi: 10.18429/JACoW-IPAC2022-MOPLXGD1
- [6] F. Zimmermann, “FCC-ee Feasibility Study Progress”, in *Proc. eeFACT’22*, Frascati, Italy, 2022, paper MOXAT0104, this workshop.
- [7] Y. Li, “Towards CEPC TDR”, in *Proc. eeFACT’22*, Frascati, Italy, 2022, paper MOXAT0105, this workshop.
- [8] C. Montag, “eRHIC- an Electron-Ion Collider at BNL”, in *Proc. SPIN’18*, Ferrara, Italy, 10-14 September, 2018.
doi:10.22323/1.346.0158
- [9] T. Satogata, “EIC Electron-Ion Collider,” presented at *eeFACT’22*, Frascati, Italy, 2022, unpublished.
- [10] A. W. Chao, K. H. Mess, M Tigner, and F. Zimmermann, Eds., *Handb. Accel. Phys. Eng.*, Sec. 3.3.9.1, pp. 287, 2nd Ed, 2013.
doi:10.1142/8543
- [11] A. W. Chao, K. H. Mess, M Tigner, and F. Zimmermann, Eds., *Handb. Accel. Phys. Eng.*, Sec. 2.4.12, pp. 155, 2nd Ed, 2013.
doi:10.1142/8543
- [12] A. W. Chao, K. H. Mess, M Tigner, and F. Zimmermann, Eds., *Handb. Accel. Phys. Eng.*, Sec. 3.3.3, pp. 273, 2nd Ed, 2013.
doi:10.1142/8543
- [13] A. W. Chao, K. H. Mess, M Tigner, and F. Zimmermann, Eds., *Handb. Accel. Phys. Eng.*, Sec. 2.5.3.2, pp. 177, 2nd Ed, 2013.
doi:10.1142/8543
- [14] E. Paterson, Private communication.
- [15] M. Sands, *The Physics of Electron Storage Rings an Introduction*, SLAC-121, UC-28, 1969, pp. 141-147.